UNIVERSITY OF OKLAHOMA

GRADUATE COLLEGE

NEW METHODOLOGY FOR INSPECTING RULED AND FREE-FORM SURFACE

IN METROLOGY

A THESIS

SUBMITTED TO THE GRADUATE FACULTY

in partial fulfillment of the requirements for the

Degree of

MASTER OF SCIENCE

By

THILLAIARASU VENUGOPAL
Norman, Oklahoma
2018

NEW METHODOLOGY FOR INSPECTING RULED AND FREE-FORM SURFACE

IN METROLOGY

A THESIS APPROVED FOR THE
SCHOOL OF INDUSTRIAL AND SYSTEMS ENGINEERING

BY

Dr. Shivakumar Raman, Chair

Dr. Janet K. Allen

Dr. Theodore Trafalis

This thesis work is dedicated to my beloved family and friends. And to my graduate advisor, Dr. Shivakumar Raman, for his support and encouragement has propelled me to reach the completion stage of my thesis.

Acknowledgements

I would like to express my heartfelt thanks to my advisor, Dr. Shivakumar Raman, who have supported me in completing this research work. It has been a great journey of almost two and half years since the day I stepped into his office to express my wish to contribute my ideas in the field of metrology.

I would also like to thank Dr. Theodore Trafalis and Dr. Janet K. Allen for being part of my thesis committee. Additionally, I would like to thank Dr. Allen for strengthening my basics in systems engineering through her graduate course. I would also like to express my gratitude to ISE faculty and staff for their contributions to my academic success. Special thanks to Dr. Kuang-Hua Chang for his Computer Integrated Manufacturing course that has helped me in understanding the fundamental concepts for my thesis work. I would like to thank Vasanth Arulprakasam, my friend who has always been the most supportive person and has provided much feedback in completing my thesis.

Finally, I express my love and gratefulness to family Amma, Appa and my brother & friend Kalicharan Venugopal. Last but not the least I wish to thank nature and friends who have supported me through highs and lows of my graduate life.

Table of Contents

List of Tables

List of Figures

x

Abstract

A new method is proposed to find the cutter contact (CC) points for both 3- and 5-axis CNC machining, and use this to determine measurement points using CMM. The first part of this research focuses on deriving a mathematical formulation to determine the CC points while using ball nose end mills and standard end mills to machine a given ruled surface, with a focus on surface finish operation. Then, the freeform surface is measured, using the Gaussian curvature and mean curvature at each grid point. These measurements at each grid point on the free-form surface are classified then into concave, convex, or saddle point surface. This way boundary surfaces are allowed to vary. This allows for a more accurate way to measure free form surfaces by distributing sample points within each boundary patch (rather than rectangular or square patches as is conventional). This will help the determination of upper and lower boundary for each patch, so that the free form surface is accurately measured. Simple experimental verification was done to demonstrate the validity of methods developed.

Chapter 1: Introduction

1.1 Machining

Roughing processes in machining are focused on a high rate of material removal, while finishing operations must produce fine finished and tight tolerances.

In CNC machines, the selected tool will follow cutter contact points generated by the machine in an ordered fashion to remove material. This process of following the CC points in removing the material for machining is called tool topology (Lasemi, Xue, and Gu, 2010). This process of connecting the CC points in an ordered manner will affect the machining time (Zhou, Zhao, and Li, 2015) and cost of machining of the product. Apart from this most widely used method, the tool path generation is affected by other parameters such as step over, scallop height, constant Z-axis usage (Z. Lin, Fu, Shen, Gan, and Yue, 2015).
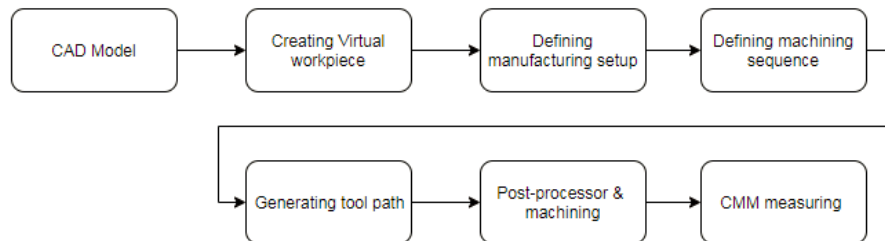
Figure 1. Machining process

1.2 Types of CNC machine

In many small and medium scale manufacturing industries, often 3-axis and 5-axis CNC machines are most commonly used. A typical machining sequence from model to inspected data is illustrated in Figure 1. In 3-axis CNC machine only X, Y, Z

are controlled, but in 5-axis machines two additional movements (rotation and tilt) are also controlled in addition to the 3-axis.

1.3 Tool path method

In the directional parallel method, the toolpath generated is parallel to the reference line and the reference line is taken on the boundary of the machined product. The counter parallel method, the tool path is generated parallel to each other in a continuous inward manner (T. Chen and Shi, 2008). For the constant step-over method, the distance the tool moves for each turn made is constant, and this is often the default method used in Computer Aided Manufacturing (CAM) packages. Its biggest advantage is the finish looks very even all over the surface. However, there is a disadvantage that if there is a high load on the corners, the toolpath generation is difficult, and the finish is compromised. So there is always a tradeoff between the type of method used and the quality of the surface finish generated (Z. Lin et al., 2015).

The other less widely used method is a Space-Filling Curve (SFC). In this method the tool path is generated with focus on reducing the length of the tool path traveling in a given direction. So, it has the disadvantage of having numerous turns on the machine surface, and the quality of the surface finish is not good when compared to other methods.

1.4 Problem statement

In this work the main goal is to find the cutter contact point of the machined surface and develop a new method for measuring the free form surface using surface partition. In the surface finish operation, the cutter will follow the path generated by the

CAM software based on the defined parametric U and W direction with constant step over. Measuring the free form surface is time consuming. In prior research the sample points were often distributed randomly in between the upper and lower boundary rectangular block and the sample points are optimized in order to reduce the measuring time. In this thesis the free surface is partitioned based on the Gaussian and mean curvature at each point in the free form surface in order to measure it.

The ruled and free form surface is converted into a parametric equation, and by using the model created, the cutter contact and the cutter location for 3-axis and 5-axis CNC machines are found at the constant U and W direction. The cutter contact and cutter location are determined for the ball nose cutter and the model is validated with the CL points generated by the CAM software.

The free-form surface converted to parametric equation is used, and the Gaussian and mean curvature values are found for each grid point. To avoid multiple patches on the surface, the curvature points are grouped into concave, convex and saddle.

Experimental validation is carried out on the 3 different sample free form surfaces. It was observed that the method developed successfully divides and groups the surface into concave, convex and saddle region.

In chapter 1 the importance of machining and various types of CNC machines are discussed. In chapter 2 the various parameters that affect the machining process and the importance of coordinate measuring machines (CMMs) in measuring ruled and free form surfaces is discussed. In chapter 3, development of new methodology in finding the cutter contact point for given surface using ball nose and end mill cutter in finishing

operation is discussed. In chapter 4, the practical implementation in measuring the freeform surface by converting the surface into three regions based on the Gaussian curvature and mean curvature is discussed. Chapter 5 details inferences and highlights the future scope of the project.

Chapter 2: Related Work and Literature Review

2.1 Machining parameters

In machining processes that focus on surface finishing, often different tools are used to remove the material. Parameters for good surface finish include step depth, step over, type of tool, and tool diameter.

2.1.1 Step depth

The step depth denotes how much in-depth the tool can plunge into the surface in a single pass. General rule of thumb is that the step depth should be less than of the tool radius. Step depth is affected by type of cutter – coating, size of the cutter, etc. (Chang, 2015)

2.1.2 Step Over

Step over depends on the quality of the surface finish we need and the cutter diameter. It is a rule of thumb that step over is usually kept at 80% of the tool diameter.(Chang, 2015)

2.1.3 Feed rate

Feed rate (F) is defined as the rate at which the material is removed. Feed rate is measured as given below:

$$F = Ft *N*n \qquad (2)$$

Ft is the feed rate per teeth for the cutter and N is the spindle speed, and n is the number of the tooth

2.1.4 Scallop height

Scallop is the amount of material which is left unmachined between two parallel tool passes. It is the difference between the designed surface and the machined surface.

Stepover and the tool diameter have an influence over the scallop height (Liu, Zhou, and An, 2012).

2.1.5 Spindle speed

Another critical parameter which will profoundly impact the surface finish is spindle speed. N denotes spindle speed measured in RPM.

$$N = V / 3.142*D \qquad (1)$$

Where V is the cutting speed of the tool in (inch/min), and D is the diameter of the cutter in inches. In addition to these tool parameters, the type of tool material may also affect the machining characteristics. Carbide tools for instance are used for the machining of high strength materials such as hardened steels and nickel-based alloys.

2.2 Tool for surface finish

Most commonly used tools in machining freeform and sculptured surfaces are the ball end mill cutter. It is beneficial to use a single tool for surface finishing operations. There are various factors that decides tool selection: surface curvature, type of surface finish, and time needed for machining.

2.2.1 Ball nose cutter

Ball nose (Figure 4), cutter is frequently used in surface finish operation. The rule of thumb in choosing the ball nose cutter is to avoid local gouging and that is to increase cutter curvature to more than the maximum normal curvature of the machined surface. (Byoung K. Choi,1998)

2.2.2 Endmill cutter

End mill (Figure 2), cutter is used in surface finish operations for pocketing, slotting, and edge finishing. The criteria in selecting the endmill cutter is that the cutter

curvature is larger than the maximum normal curvature of the surface that needs to be machined.(Li & Zhang, 2004).

2.3 Tool path method

By considering all the parameters, the tool path is classified based on the quality, efficiency, and robustness. The primary objective of tool path generation is to connect all the cutter locations. This process is done two ways - one is by using cutter contact (CC) method, and the other is by the cutter location (CL) method. The primary aim of these two methods is to get smaller scallop height with shorter tool paths in machining that results in less cost and less machining time.

In CC based method, CC points are produced based on the designed machine surface, and then it will be converted to CL points. This CC based method is used in PRO-E®. This method is further classified into three types: parametric method, guide plane, and drive surface (Chang, 2015). In the parametric method, there is a drawback of getting nonuniform scallop height because in the process of converting the parametric to Euclidian space an error results in non-uniform scallop height (Y. J. Lin & Lee, 1999). In drive surface method, the tool path is derived by connecting the design surface with many planes known as drive surfaces and this curve in the design surface are connected to form a tool path. This method is suitable for the very complex surfaces. Guide plane method is not used as much since it can only be applied to 3-axis machining (Xu & Newman, 2006). All the three methods in CC based tool path generation are explained.

In CL based tool path generation method, CL surface needs to be generated from the machining surface during the design phase, and the difference is that the offset is

first generated, and then the tool path is generated on the offset surface which helps in providing good surface finish.
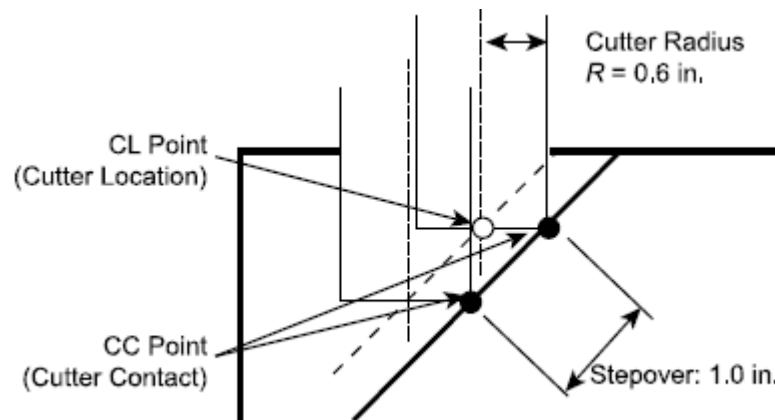
Figure 2. CL and CC offset for flat end mill cutter in 45 deg surface (Chang, 2015)

Typical cutter contact, and cutter location point are shown in Figure 2. For this example, flat end mill cutter used, and the CL point does not intersect the CC point and the surface radius of the cutter used is 0.6 inch and this machining done on 3-axis machining on a 45*inclined plane, and the step over was taken as 1 inch.

As the CC and CL line not on the same point, there will large amounts of material left unmachined.

8
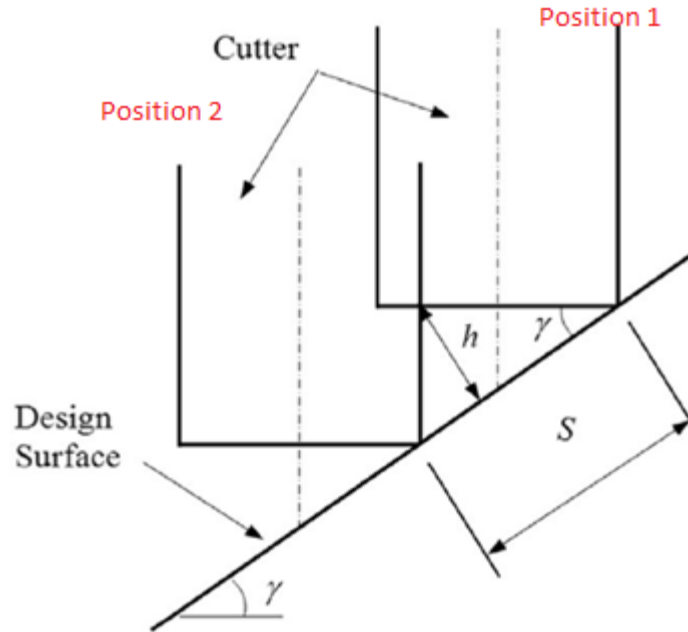
Figure. 3 Scallop parameters (Chang,2015)

In this case, the scallop height can be calculated by

$$H = S * (\cos \gamma) * \sin \gamma \qquad (3)$$

Where H is the scallop height and γ is the slope angle of the design surface shown in Figure 3. If we use the ball nose cutter for the same condition, the CC and CL will coincide with each other. So, tool selection and the type of CNC axis selected affects surface finish.

In ball nose cutter, the CL points is offset in Y and Z direction for 3-axis. The offset is calculated by

$$O_y = R * \sin \gamma \qquad (4)$$

$$O_z = R * (1 - \cos \gamma) \qquad (5)$$

Once the offset calculated, we can find the CL for X, Y and Z direction using the formula given below,
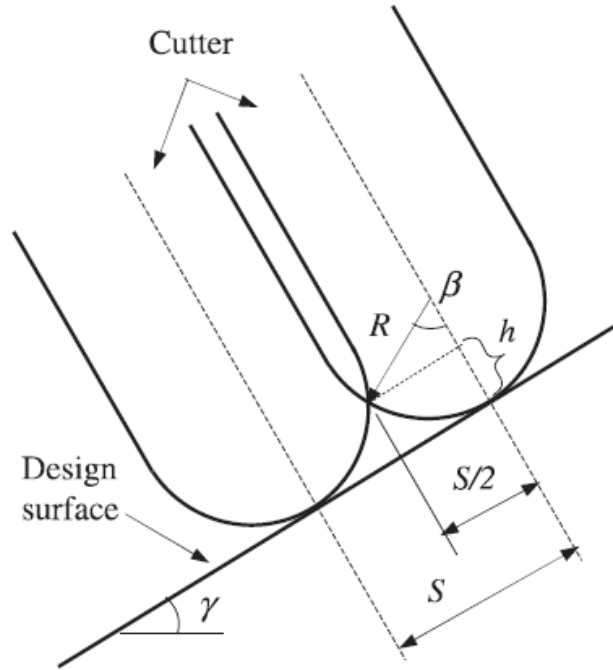
Figure 4. Tool orientation for ball nose in 5-axis CNC. (Chang, 2015)

$$CL_x = CC_x \qquad (6)$$

$$CL_y = CC_y - O_y \qquad (7)$$

$$CL_z = CC_z - O_z \qquad (8)$$

The main aim of a tool path is to improve the efficiency of the tool run and quality of the surface finish. They are broadly classified into two main types as: 1) Tool path generation based on the machining strip method and 2) Region-based free surface. Apart from this are many research works based on the tool path generated for the freeform surface.

In the paper by (Ding, 2003) an analogy is drawn from lawn moving, where the free form surface is taken as a lawn with planted grass and the cutter must pass through the given tool path to cut the grass. Two approaches are suggested (ElKott, 2007). The

first step is the cutter toolpath placed in the cutter contact point on the surface and series of grass ring formed. Then this is converted into parametric view to calculate the next tool path. This process continues till the whole surface is covered in the machining software (Shunmugam, 1987).However, the method proposed is suitable only for the larger diameter cutter. In case where a smaller diameter cutter is used for better surface finish, the toolpath generation could become time-consuming, resulting in high machining time.

2.4 CMM measurement

Measurement errors plays an important role in finding the actual dimension of the machined surface. CMM plays an important role in finding the dimension. CMM has a ruby ball which is attached to the machine which has two main errors one is probe compensation error and probe travel error. Apart from this there is a surface fitting error which occur during fitting the data points to recreate the model.

2.5 Surface parameters

2.5.1 Gaussian curvature

Gaussian curvature is the product of the two-principle curvatures K_1 and K_2. It has high importance in finding the curvature of the surface at a point P. The Gaussian curvature is an intrinsic measure of the surface.

2.5.2 Mean curvature

Mean curvature is the average of the two-principal curvature K_1 and K_2. And it is considered as an extrinsic measure of the surface at a given point P.

11

2.6 Surface partition

In the traditional machining, the tool path generated for the whole material region is treated as one. However, due to the complexity of the machining surface and maintaining the feed direction for getting the maximum strip and machining efficiency, in (Zhou et al., 2015) they have proposed a new method of dividing the complex surface into multiple sub-regions. The tool path is generated for each sub-region of the same material and helps to attain the regional machining surface and tensor machining property used for both the tool path generation and region subdivision for machining. They explained how to divide the complex surface into multiple sub-regions and to generate the tool path. They did not explain the critical point which will determine how to separate the complex surface into different sub-regions, and they did not explain how to implement this method for other complex free-form surfaces. In research by (Lasemi et al., 2010) they have given information about the recent developments in machining CNC freeform surfaces with main focus on tool geometry, tool orientation and toolpath generation.

In (Z. C. Chen, Dong, & Vickers, 2003) the most important surface parameters such as K and H are considered to subdivide the entire freeform surface into subgroups. Here they used this method for roughing operation and grouped into convex, concave and saddle surfaces. Then the C-mean, Fuzzy clustering method is used to optimize the surface partition. However, there is a disadvantage in this method; the free form surface is subdivided to form too many patches.

In (Roman, Bedi, & Ismail, 2006) the free form surface is subdivided into larger patches so there are fewer patches compared to (Z. C. Chen et al., 2003) . Here they

have used the K-means clustering algorithm for surface subdivision however this method also has a patch range from 1 to 15 which still considered as many patches which is based on how easy to machine to surface and tool orientation needed for each patch. In (Radzevich, 2007) they have used a focal surface for surface partition. However, this method is not applicable for all kinds of sculptured surface. In (Park and Choi, 2001), they have tried with the Z-map model. Using this model, they could extract the features like pockets, uncut and contour regions but it is difficult to get the Z-type model for a smooth free surface.

Many challenges such as machining quality and efficiency need to be addressed. The new concept of curvature matched machining has an advantage over other methods like the Iso-scallop method. Moreover, there is always a tradeoff between the machined quality and machining surface. This issue is due to many factors such as tool selection, feed rate, type of machining surface, and tool path generation algorithm.

Much research has been carried out in field of surface partition. Most the surface partition work is done in the field of machining and very few works have been taken in the field of metrology.

In this work, we have introduced a new method to divide the surface into 3 regions with fewer number patches based on the Gaussian and mean curvature.

Chapter 3: Methodology

3.1 Methodology

In this paper, mathematical formulation is derived for the CC points and CL points determination. To find the relation between each parameter the tool orientation and axis orientation are studied in detail and the mathematical model is verified with PROE®.

In mathematical modelling, we will initially convert the ruled surface into parametric form for getting a clear understanding of the ruled surface

The overall methodology is explained below.

1. Ruled surface model is created using SOLIDWORKS®.

2. CAMWorks® is used to sequence the machining process.

3. Parts are manufactured using 3-axis milling machine.

4. CL data points are determined using the formulation, based on the type of cutting tool

5.   MATLAB® is used to form the parametric surface and a program is used to classify the grid points based on the Gaussian and mean curvature

6.   CMM is used to measure the machined parts and compare it with the ideal point

7. Sculptured parts are created to validate the model
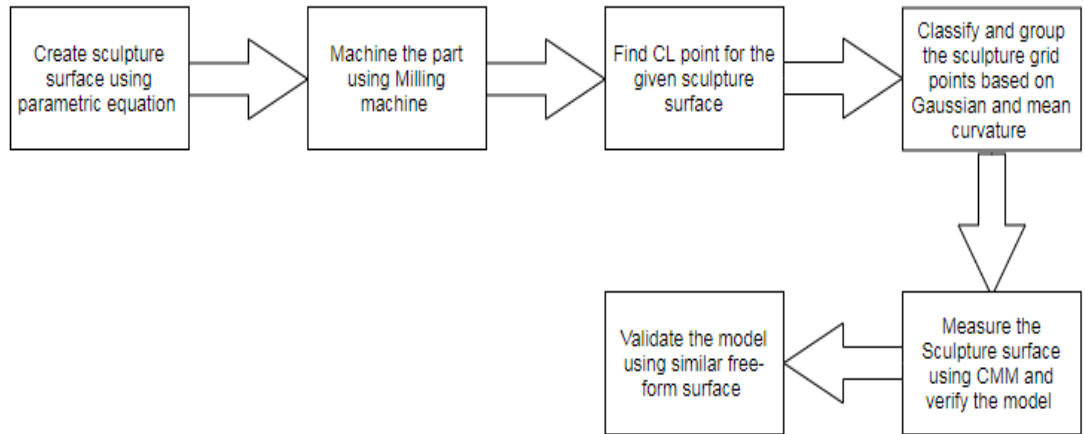
Figure 5. Surface partition algorithm
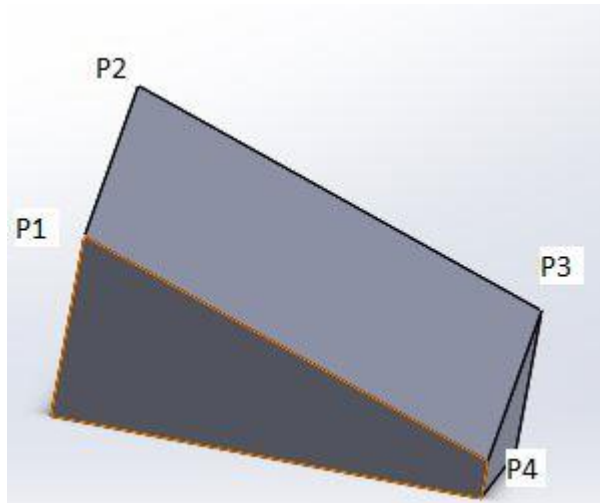
Figure 6. Ruled surface -PROE CREO®-CAD model

The ruled part which needs to be machined is 4-inch-wide on one side and is 5-inch wide on the other end which as shown in the Figure 5. The length of the edge, P_1P_2, is taken as D_{12}, and the length of the edge P_3P_4 is taken as D_{34}.

$$D_{12} = \sqrt{4^2 + 0^2} \qquad\qquad = 2 \text{ inch}$$

$$D_{34} = \sqrt{4^2 + 5^2} \qquad\qquad = 3 \text{ inch}$$

The scallop height (H) can be calculated by

$$H = R*(1- \cos \beta) \quad (9)$$

$$\beta = \text{Sin}^{-1} (S/ 2*R) \quad (10)$$

$$S_{34} = D_{34} / (\text{number of passes} -1) \quad (11)$$

$$S_{12} = D_{12} / (\text{number of passes} -1) \quad (12)$$

The step-over between each pass by cutter is denoted by S.

PROE-CREO® creates the number of passes based on the midplane to reduce the scallop difference between the front and the back edge of the model. However, if the scallop is specified the number of passes, N, can be calculated by

$$N = (D_m /S) +1 \quad (13)$$

3.2 Mathematical formulation

For parametric conversion, first we need to convert the ruled surface into parametric form hence the X, Y, Z coordinates are converted into U and W parameter space, where U $\in$ [0,1] and W $\in$ [0,1]. The parametric representation of the Cartesian coordination of any point on the surface can found by this, and widely used and it will help us in getting the parametric values in the form of U and W.

Let P_1, P_2 be the points in the space, the parametric representation in the straight line is given by

$$P(U) = P_x(U), P_y(U), P_z (U) \quad (14)$$

$$= (1-U) *P_1+U*P_2 = (1-U) * [P_{1x}\ P_{1y}\ P_{1z}] + U*[P_{2x}\ P_{2y}\ P_{2z}] \quad (15)$$

As the points in U $\in$ [0,1] equation 15 will become

$$P(U) = (1-U) *P_1 +P_2*U \quad (16)$$

$$Q(U) = (1-U) *P_3 + P_4*U \quad (17)$$

By substituting in the equation, the points for parametric equation is

16

$$P_1 = (0,0,0) \qquad P_2 = (0,4,0)$$

$$P_3 = (10,0,-5) \qquad P_4 = (10,4,0)$$

The parametric equation for the given ruled surface in S (U, W) is

$$S (U, W) = [S_x (U, W), S_y (U, W), S_z (U, W)]$$

$$= P(U) + W*[Q(U)- P(U)]$$

$$= (1-W) *P(U) + W *Q(U)$$

$$= (1-W) [(1-U) *P_1 +U*P_{2]} + W * [(1-U) *P_3 +U*P_4] \qquad (18)$$

$$S (U_i,W_j)= (1-W_j) [(1-U_i)*P_1 +U_i*P_2] + W_j * [(1-U_i)*P_3 +U_i*P_4] \quad (19)$$

By using equation 18 we can find the Cartesian coordinates.

For our model by substituting the points P_1, P_2, P_3, P_4 the Cartesian equation can be found from equation 18,

$$S (U, W) = (10W, 4U, 5UW - 5 W) \qquad (20)$$

This equation, the CC lines are formed as straight lines. We can find the points Pi at any line of the CC points, and the respective U and W coordinates can found. Then the cutter orientation can also be found using the same way, and the normalized vector of the given parametric surface.

$$N_n = (T_w *T_U) / | T_w *T_U| \qquad (21)$$

T_w = Tangent vector of the surface in W direction

T_u = Tangent vector of the surface in U direction

So, the tangent vector can be found by

$$T_w= S (U, W), W = ðS (U, W) / ðW \qquad (22)$$

$$T_u= S (U, W), U = ðS (U, W) / ðU \qquad (23)$$

Therefore $T_w = [10, 0, 5U - 5]$

$$T_U = [0, 4, 5W]$$

So, $N_n = (T_w * T_U) / |T_w * T_U|$

$$T_w * T_U = \begin{vmatrix} i & j & k \\ 10 & 0 & 5U - 5 \\ 0 & 4 & 5W \end{vmatrix}$$

$$T_w * T_U = [-20U + 20, -50W, 40] \qquad (24)$$

Equation 24 will give a tangent point of the tool on the surface at any point in the ruled surface.

3.3 CC point and tool orientation calculation for 5-axis CNC ball nose

For 5 -axis CNC the CC and CL points will coincide regardless of the tool used.

So, the $CC_X = CL_X$, $CC_Y = CL_Y$, $CC_Z = CL_Z$

So, from the equation 19

$$CC_X = 10W, CC_Y = 4U, CC_Z = 5WU - 5W$$

And the tool orientation for 5-axis ball nose end mill cutters is

$$N_x = \frac{-20U + 20}{\sqrt{(-20U + 20)2 + (-50U)2 + (40)2}}$$

$$N_y = \frac{-50W}{\sqrt{(-20U + 20)2 + (-50U)2 + (40)2}}$$

$$N_z = \frac{40}{\sqrt{(-20U + 20)2 + (-50U)2 + (40)2}}$$

3.4 CC point and tool orientation calculation for 3-axis CNC ball nose
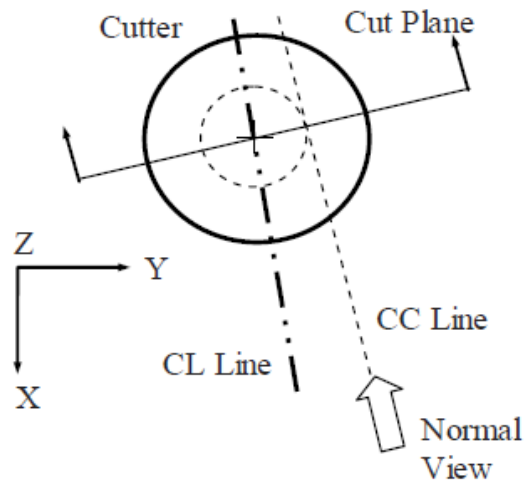
Figure 7. Tool offset for 3-axis ball-nose cutter (Obeidat, 2008)

In 3 axis ball nose cutters, the CC points and CL point do not coincide. Hence, we could see the tool is offset in X and Y direction but not in Z direction as the Z direction is always normal.

$$CC_X = 10W, CC_Y = 4U, CC_Z = 5WU - 5W$$
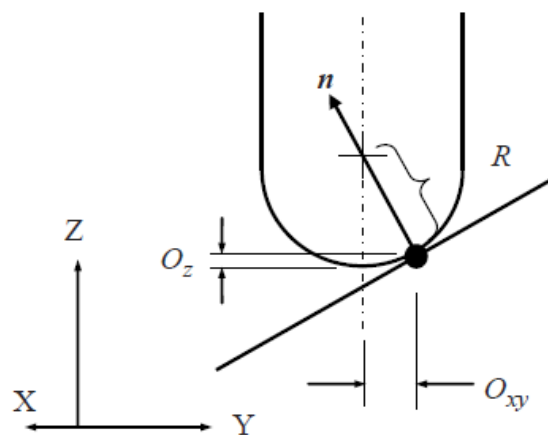
Figure 8. Tool offset on an inclined plane (Chang, 2015)

The CL point is offset from CC point by

$$O_X = R * N_x$$

$$O_Y = R * N_y$$

$$O_Z = R * (1-N_z)$$

Moreover, the Cl data is obtained by

$$CL_X = CC_X + O_X$$

$$CL_Y = CC_Y + O_y$$

$$CL_Z = CC_Z + O_Z$$

3.5 CC point and tool orientation calculation for 3-axis CNC endmill

The ball nose cutter in 3-axis the end mill cutter has offset, and it can be found by the following

$$CC_X = 10W, CC_Y = 4U, CC_Z = 5WU- 5W$$

The below equation finds the tool orientation

$$N_x = \frac{-20U+20}{\sqrt{(-20U+20)2+(-50U)2+(40)2}} \quad O_x = \frac{RNx}{\sqrt{Nx2+Ny2}}$$

$$N_y = \frac{-50W}{\sqrt{(-20U+20)2+(-50U)2+(40)2}} \quad O_y = \frac{RNy}{\sqrt{Nx2+Ny2}}$$

$$N_z = \frac{40}{\sqrt{(-20U+20)2+(-50U)2+(40)2}} \quad O_z = \frac{RNy}{\sqrt{Nx2+Ny2}}$$

$$CL_X = CC_X + O_X \qquad CL_y = CC_y + O_y \qquad CL_Z = CC_Z$$

These equations help in generating the CC and CL points in CNC machine based on the type of tool used and axis which is used for the machining. for this experiment the common parameters for the tool path generation validation is given below.

3.6 Boundary conditions and parameters

The below table was used as the parameter for the machining the part in PROE CREO® for 3 and 5 axis CNC Milling machines.

Table 1: Parameters for Machining process

Parameter	Unit
Stepover	1 inch
Tolerance	.001 inch
Clear distance	1 inch
Spindle speed	2000 rpm
Tool diameter	1.2 inch
feed rate	10 inch/ min

The results of finding the CC points an CL points for the given model is given in the below Table 2, Table 3 and Table 4. Then the points are cross verified with PROE-CREO® model.

Chapter 4: Experiment and Results

For verification, here we have taken the U and W value varied from 0 to 1. By using the range of U and W values, the CL and CC points of the tool based on CNC machine are found. From the PROE® result, by comparing the CC_X, CC_Y, CC_Z and tool orientation, we find that the X,Y,Z points coincide with the CL data at various U and W positions. By using the different values of U and W we can get the entire CC, CL points for the given surface.

Table 2:   5-axis ball-nose cutter with CC_X, CC_Y, CC_Z

u	w	CCx	CCy	CCz	nx	ny	nz
1.00	0.00	0	4	0	0	0	1
1.00	0.16	1.6	4	0	0	-0.1961	0.9805807
0.75	0.875	8.75	3	-1.094	0.08405	-0.73542	0.6723817
0.75	0.47	4.7	3	-0.588	0.10716	-0.50363	0.8572467
0.75	0.563	5.63	3	-0.704	0.10169	-0.57254	0.813549
0.5	0.38	3.8	2	-0.95	0.22027	-0.41852	0.8810915
0.5	0.281	2.81	2	-0.703	0.22957	-0.32255	0.9182909
0	1	10	0	-5	0.29814	-0.74536	0.5962848

As tool orientation plays a role, it will have an impact on the cutter contact with the free form surface and the cutter orientation will not be same as the 5- axis CNC machine as the 3-axis machine.

Table :3   3-axis ball-nose cutter by comparing the CLx, CLY, CLz

u	w	CCx	CCy	CCz	nx	ny	nz	Ox	Oy	Oz	CLx	CLy	CLz
1.00	0.00	0.00	4.00	0.00	0.00	0.00	1.00	0.00	0.00	0.00	0.00	4.00	0.00
1.00	0.15	1.50	4.00	0.00	0.00	-0.18	0.98	0.00	-0.11	-0.01	1.50	3.89	-0.01
1.00	0.50	5.00	4.00	0.00	0.00	-0.53	0.85	0.00	-0.32	-0.09	5.00	3.68	-0.09
0.75	0.47	4.72	3.00	-0.59	0.11	-0.51	0.86	0.06	-0.30	-0.09	4.78	2.70	-0.68
0.50	0.47	4.69	2.00	-1.17	0.21	-0.49	0.84	0.13	-0.30	-0.09	4.82	1.70	-1.27
0.50	0.56	5.62	2.00	-1.41	0.20	-0.56	0.80	0.12	-0.34	-0.12	5.74	1.66	-1.52
0.25	0.56	5.63	1.00	-2.11	0.29	-0.55	0.78	0.18	-0.33	-0.13	5.81	0.67	-2.24
0.00	0.00	0.00	0.00	0.00	0.45	0.00	0.89	0.27	0.00	-0.06	0.27	0.00	-0.06
0.00	1.00	10.00	0.00	-5.00	0.30	-0.75	0.60	0.18	-0.45	-0.24	10.18	-0.45	-5.24

Table :4   3-axis flat-endmill cutter by comparing the CLx, CLY, CLz positions

u	w	CCx	CCy	CCz	nx	ny	nz	Ox	Oy	CLx	CLy	CLz
0	1	10	0	-5	0.29814	-0.7454	0.59628	0.2228	-0.55709	10.2228	-0.5571	-5
1	1	10	4	0	0	-0.7809	0.6247	0	-0.6	10	3.4	0
0.75	1.00	10	3	-1.257	0.07757	-0.7803	0.62055	0.0594	-0.59706	10.1191	2.4029	-1.25746
0.75	0.875	8.8	3	-1.094	0.08405	-0.7354	0.67238	0.0681	-0.59612	8.81813	2.4039	-1.09375
0.75	0.625	6.3	3	-0.781	0.09803	-0.6127	0.78423	0.0948	-0.59246	6.34479	2.4075	-0.78125
0.5	0.185	1.9	2	-0.463	0.23665	-0.2189	0.94661	0.4405	-0.40743	2.29046	1.5926	-0.4625
0.5	0.281	2.8	2	-0.703	0.22957	-0.3225	0.91829	0.3479	-0.48883	3.15792	1.5112	-0.7025
0.25	0	0	1	0	0.35112	0	0.93633	0.6	0	0.6	1	0
0	0	0	0	0	0.44721	0	0.89443	0.6	0	0.6	0	0

For 3-axis CNC machine, the CL position for X, Y, Z position is also verified with PROE® model with respective U and V position in parametric method at random

position. The entire tool orientation, CC points and CL points for 3-axis and 5-axis model can be found in PROE® ". ncl "separately.

If we need to modify the CC points for any surface we can modify the number of CC points in between the lines and given as an input to MATLAB® . Using this mathematical model we can find the CC and CL point for any kind of ruled surface as well as for the freeform surface.

4.1 Converting the surface to parametric form for free-form surface

It is difficult to get the CL and CC points for the machined surface so there is need of new methodology for measuring the freeform surface.

Once we confirmed the model which we derived is accurate enough to find the cutter location points we extended this method to the freeform surface. For designing the freeform surface CAMWorks® has been used. Regarding the freeform surface, we need to convert the freeform surface into parametric form by using the CAD Software Cubic curves are formed. For this work two freeform surfaces are formed and are converted to parametric surface equation in the form of U and W. The value of U and W ranges from 0 to 3. Parametric surface equation is represented by the below equation.

$$S(u,w) = [Sx(u,w), Sy(u,w), Sz(u,w)]_{1X3}, (u,w) \in [0,3]X[0,3] \ (25)$$

The parametric curves are combined to form the free surface using the curve P, Q, R, T. Using equation 26 values are combined into matrix and surface is formed using MATLAB®

$$S(u,w) = [w^3 \; w^2 \; w \; 1] \begin{bmatrix} \begin{bmatrix} -1/6 & 1/2 & -1/2 & -1/6 \\ 1 & -15/6 & 2 & -1/2 \\ -11/6 & 3 & -3/2 & 1/3 \\ 1 & 0 & 0 & 0 \end{bmatrix} \end{bmatrix} \begin{bmatrix} P(u) \\ Q(u) \\ R(u) \\ T(u) \end{bmatrix} \quad (26)$$

The parametric equation is provided to the CAD software and the curves are lofted to form the surface in SOLIDWORKS®. CAMWorks® is used to machine the surface virtually by sequencing the machining operation (roughing and finishing). Two scruptured surfaces have been designed and 3 replicates of each are machined using 3-axis milling machine. Cutter location (CL) was derived using the CAMWorks®.

The parameters to machine all the freeform surfaces is maintained as constant for all the 3 samples.

Table 5 : Parameter for machining the free-form surface

Parameter	Sample 1	Sample 2	Sample 3
Speed (RPM)	2000	2000	2000
Feed rate (IPM)	30	30	50
Pattern	slice	slice	slice
Stepover	0.005	0.005	0.005
Allowance	0	0	0
Z allowance	0	0	0
Directional	zigzag	zigzag	zigzag
Cutter	Ball nose	Ball nose	Ball nose
Cutter diameter	.25 inch	.25 inch	.25 inch

4.2 Surface geometric parameter

As discussed in chapter 2, the parameters for finding the Gaussian and mean curvature are explained here. Here E, F G are considered as the first fundamental parts of the parameters and L,M,N are considered as the second fundamental parts (Radzevich, 2007).

"n" is considered as the unit normal vector each point on the surface S (U, W). Where S_U and S_W are the unit tangent vector in U and W direction.

E $= (\partial S/\partial u)* (\partial S/\partial u)$

F $= (\partial S/\partial u)* (\partial S/\partial v)$

G $= (\partial S/\partial v)* (\partial S/\partial v)$

L $= n*\partial^2 S /\partial u^2$

M $= n*\partial S^2 /\partial u \, \partial v$

N $= n*\partial^2 S /\partial v^2$

n $= (S_U*S_W) / | S_U *S_W |$

The Gaussian curvature K

$$K = (LN - M^2)/(EG - F^2)$$

$$K = K_{max} * K_{min}$$

The mean curvature, H is given by

$$H = \frac{1}{2} * (\frac{EN-2FM+GL}{EG-F^2})$$

$$K_{max}= H+\sqrt{(H^2 - K)}$$

K_{max} and K_{min} are the principal curvature which is given by

$$K_{max}= H+\sqrt{(H^2 - K)}$$

$$K_{min} = H - \sqrt{(H^2 - K)}$$

The free-form surfaces are formed at the regular interval from the range of 0 to 3 using MATLAB® The grid points are formed at the intersection of the lines in U and W direction.
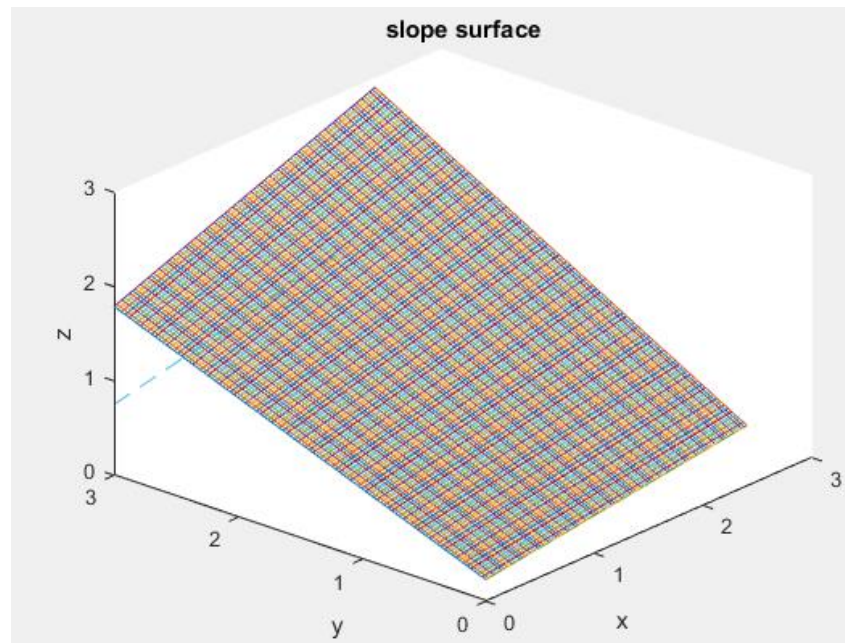
Figure 9. Parametric ruled surface
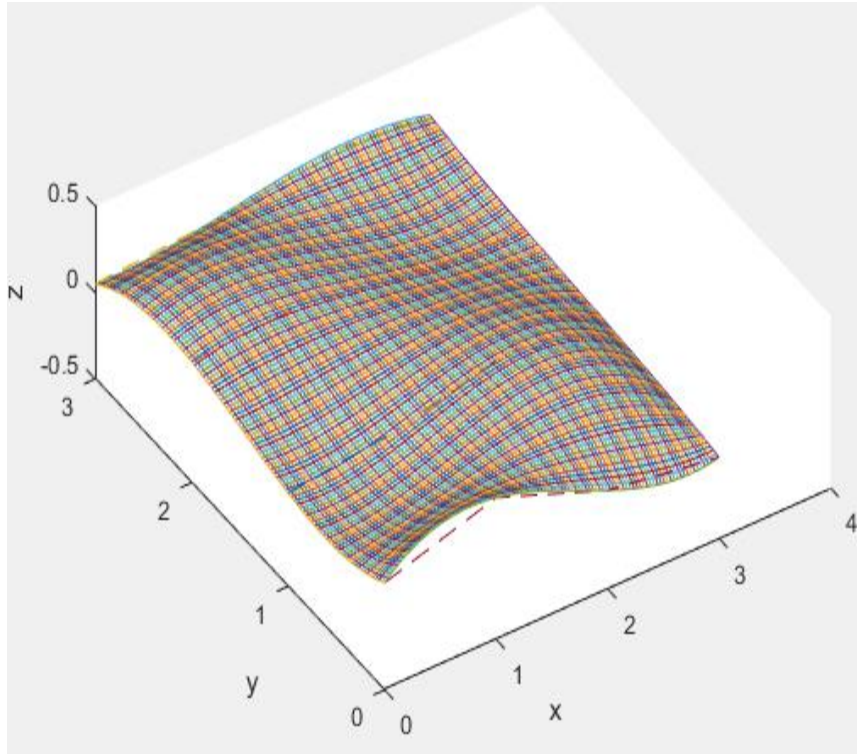
Figure 10. Parametric free-form surface 1 (Shallow)

Freeform surfaces representing the shallow and deep surfaces are shown in Figure 9 and Figure 10 and the control points for both the free form surface is at four different location and it is denoted in dotted lines in the Figure 9 and Figure 10.
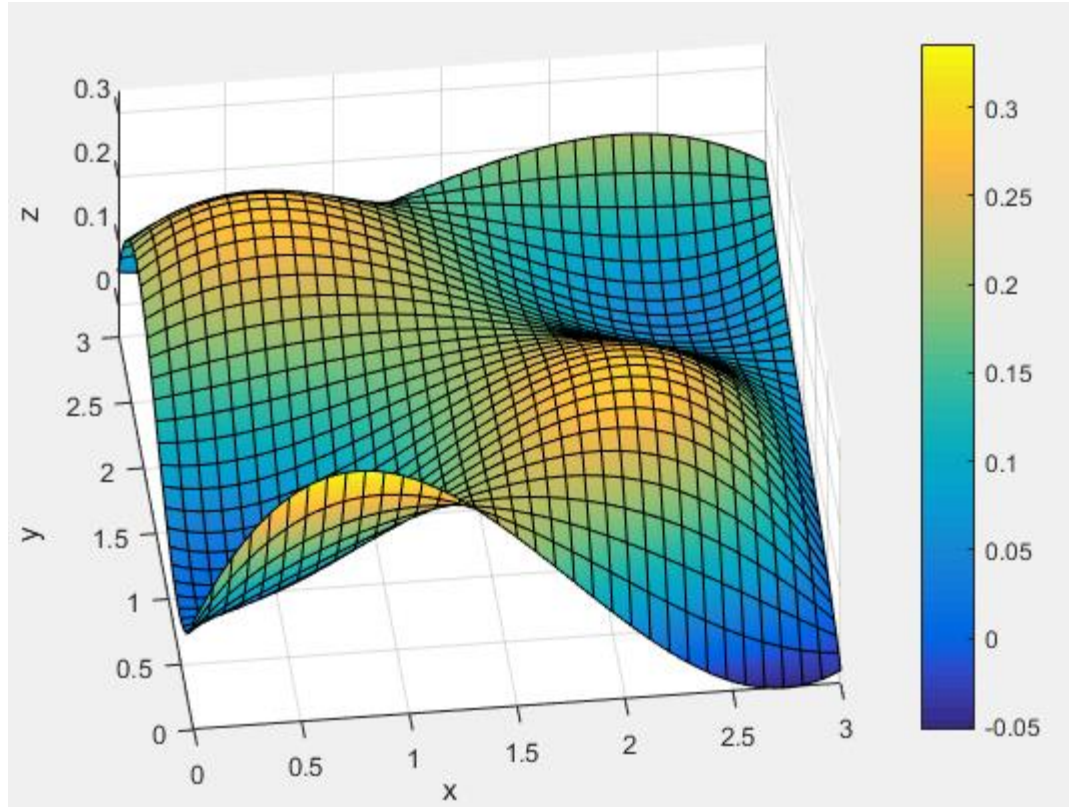
Figure 11. Parametric free form Surface 2 (Deep)

4.3 Separation model Explanation

Step 1:

Specify parametric mathematical model of the sculptured or freeform surface in the U and W directions.

Step 2:

The grid points in the U and W directions, are generated from 0 to 3.

Step 3:

The Gaussian curvature and mean curvature at every grid point intersection is calculated.

Step 4:

29

Group areas into convex, concave and saddle point.

Condition 1:

K >= 0 and H < 0: point is Convex

Condition 2

K >= 0 and H > 0: point is Concave

Condition 3:

K < 0 and H ≠ 0: point is saddle

4.4 Region seperation and conditions

The flow chart of the algorithm is shown in detail with the condition on how we separate the points in U and W direction.
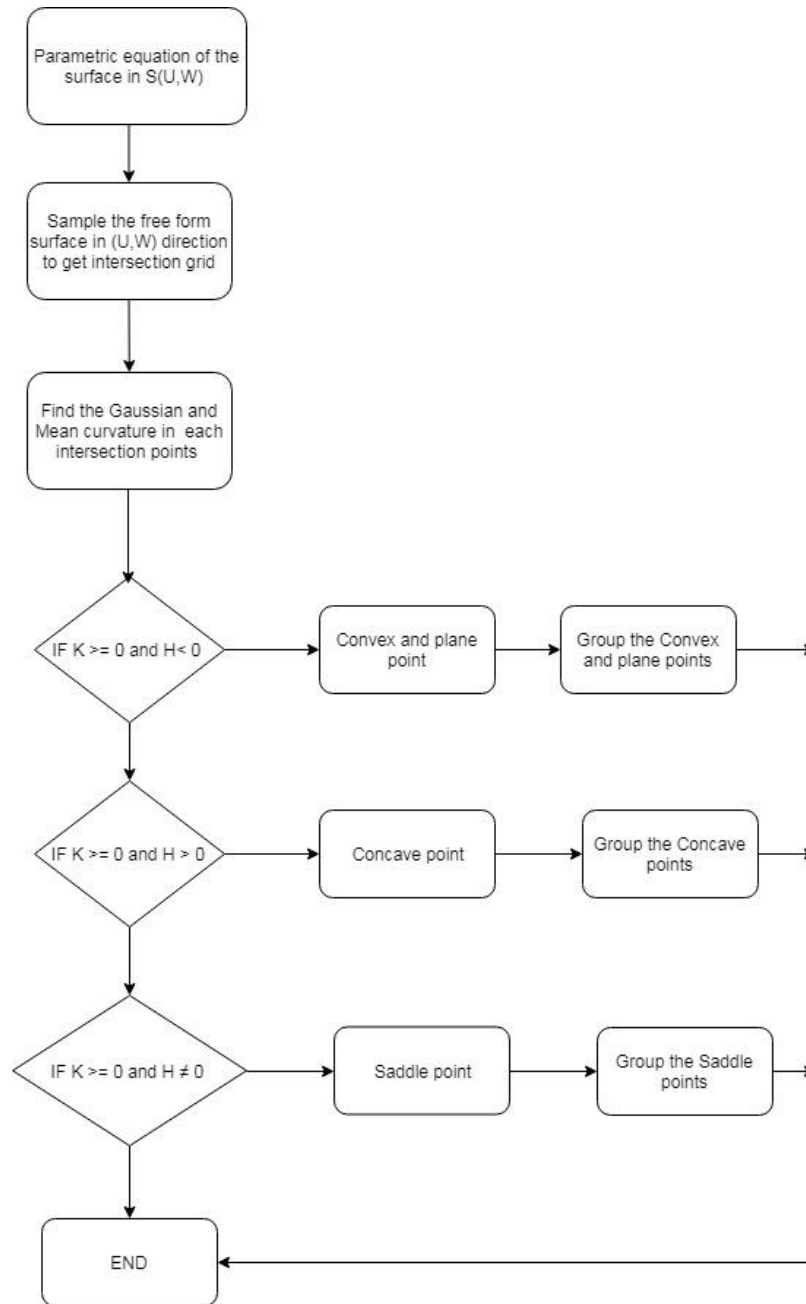
Figure 12. Overall model flow

Using MATLAB®, the Gaussian curvature and the mean curvature have been determined at each grid point and it is stored in the matrix and the sample Gaussian curvature and mean curvature matrix and values is shown in the Table 6 and Table 7. The dimension of the Matrices K and H are kept as 61*61.

Table 6. Sample Gaussian curvature matrix(K)

-0.29177	-0.25803	-0.23884	-0.23199
-0.2326	-0.20275	-0.18634	-0.18127
-0.16872	-0.14348	-0.13043	-0.1276
-0.10253	-0.08241	-0.07314	-0.07293
-0.03667	-0.02192	-0.01669	-0.01937
0.026164	0.035548	0.036692	0.03104
0.083472	0.087762	0.084986	0.076431
0.133193	0.132872	0.126528	0.11531

Table 7. Sample mean curvature matrix(H)

0.540493	0.535601	0.525763	0.512399
0.522158	0.521811	0.516968	0.508807
0.506276	0.509982	0.509435	0.50562
0.491904	0.499151	0.50224	0.502003
0.478195	0.488451	0.494554	0.497207
0.464437	0.477155	0.48568	0.490603
0.450081	0.464705	0.475089	0.481724
0.434751	0.450727	0.462436	0.470282

Then based on the values of K and H at each grid points, three different matrices

M1, M2, and M3 are formed
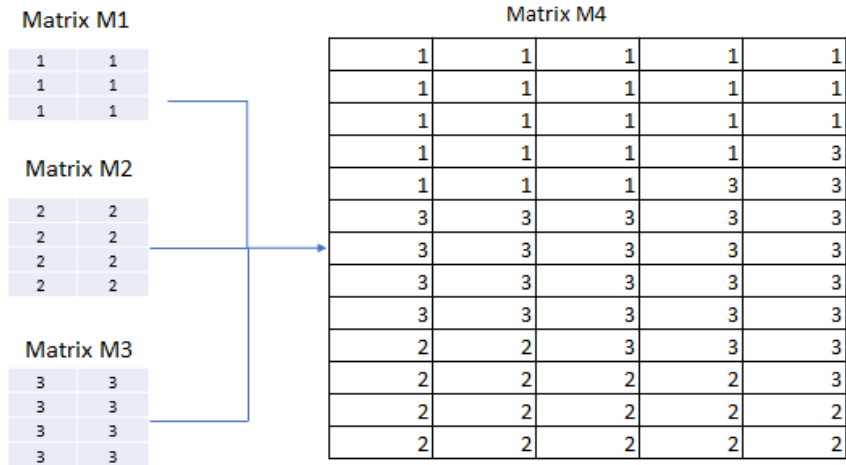
Figure 13. Matrix showing the region separation

To classify the surface, value 1 has been assigned to the matrix M1 which contain the convex and plane surface and value 2 has been assigned to the matrix M2 which contain Concave surface and value 3 to matrix M3. The Matrix M4 is formed by combining all the three matrices M1, M2, and M3 which is of same dimension as the matrices K and H.

Based on the value of the matrix M4, the surface separation is done using Excel® Conditional formatting. and the boundary is formed on the region where the values at each grid point is different. From the Table 14 and Table 15, we could see the grid points are separated based on the Gaussian and mean curvature into concave, convex, and saddle points and each grid point have the unique U and W position which is then mapped to the X, Y location of the machined surface, so that points can be measured.
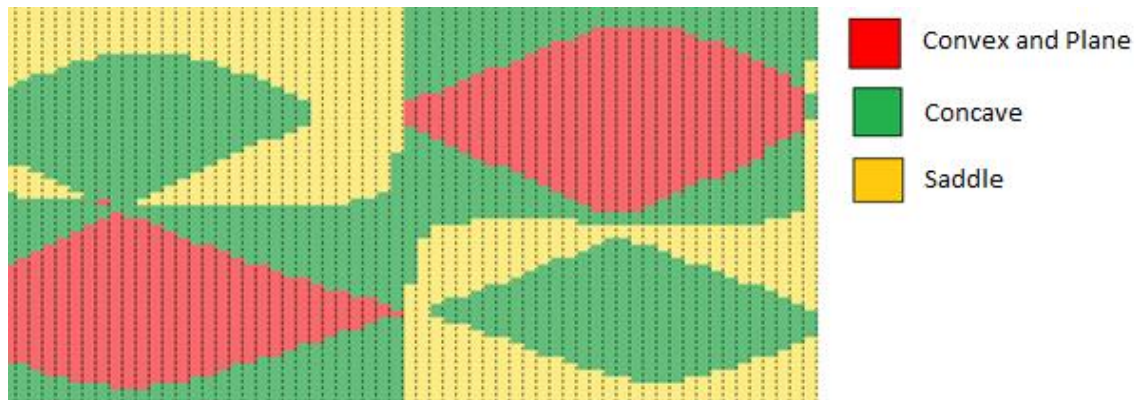
Figure 14. Boundary separation -Surface_deep

From the data points of the sculpture surface2, the surface is divided based on the values, and it is color coded based on the values assigned from 1 to 3 depending on the surface. It is found that for the given freeform surface, six patches are formed, and boundary is formed to separate the surface.

33
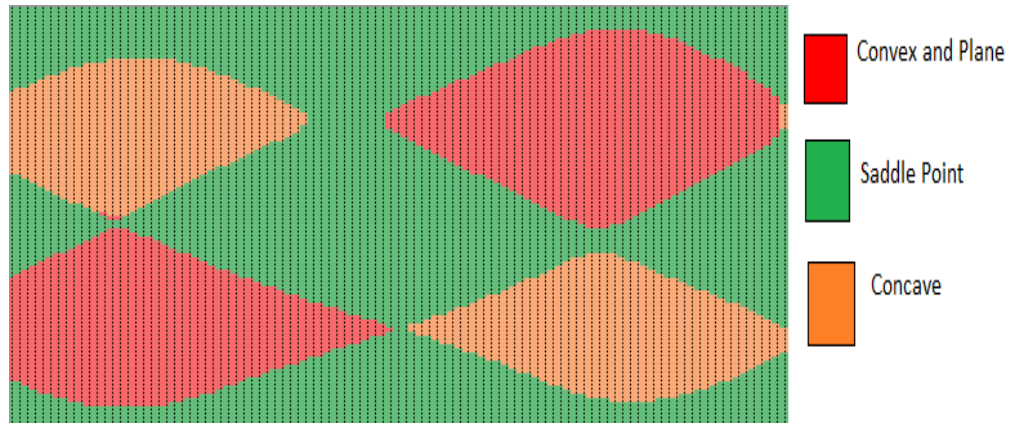
Figure 15. Boundary separation -Surface_Shallow

BROWN & SHARPE® CMM PFX454 system was used for measuring the machined aluminum-6061 surface. 4mm ruby ball probe of 30 mm length was used for all the experiments to keep the measurement error constant. The ruby ball is calibrated before measuring. PC-DMIS 2011® software was used in CMM program to inspect the points at calculated locations. To maintain the consistency all the samples were run through the same datapoint.

The test results confirm that the algorithm successfully divides the surface based on the Gaussian and mean curvature value at each grid points and the maximum error for the positive and negative side was taken into consideration and the results are in the table below.

Table 8. Maximum error between the measured and calculated points

Surface	Sample #	x (inch)	Y (inch)	z (inch)
Surface _shallow	sample 1	0.0695	0.0245	0.07
	sample 2	0.024	0.081	0.026
	sample 3	0.015	0.064	-0.012
Surface _Deep	sample 1	0.045	0.027	0.0624
	sample 2	0.0124	0.0244	0.128
	sample 3	0.045	0.0298	0.092

Chapter 5: Conclusion and future scope

In this work a new methodology for finding the cutter contact position for measuring the ruled and freeform surface has been introduced. The mathematical formula which we derived is used to find the cutter location and tool orientation for both 3-axis and 5-axis CNC machines. Here we have implemented a separate method for finding the cutter contact point for ball nose mill and standard end mill. The datapoints derived from the mathematical formulation is compared with commercial software. We can extend this work by using the CL data file to find the dimension of the part without the use of parametric equation. As the parametric equation of the complex profile is difficult to derive in real world. This establish the interconnected systems by combining the machining and measuring in production plant.

For freeform surface a new method was developed to form subgroup areas by separating the areas into concave, convex and saddle regions based on the Gaussian and mean curvature of the freeform surface. By separating the area into many sub regions, we can further optimize the measuring points based on the local area irrespective of the complex surface. This will eliminate the time in measuring the complex surface and boundary are formed based on the surface curvature not on patches.

We can extend the research work by applying aligned, random and stratified sampling techniques within each sub region, and optimizing the number of sampling points needed to calculate the form error and position of the surface and compare it with the CAD model.

References

Byoung K. Choi, R. B. J. (1998). *Sculptured Surface Machining*. SPRINGER
SCIENCE+BUSINESS MEDIA, B.V.

Chen, T., & Shi, Z. (2008). A tool path generation strategy for three-axis ball-end
milling of free-form surfaces. *Journal of Materials Processing Technology*.
https://doi.org/10.1016/j.jmatprotec.2007.12.142

Chen, Z. C., Dong, Z., & Vickers, G. W. (2003). Automated surface subdivision and
tool path generation for 3 1/2 1/2-axis CNC machining of sculptured parts.
Computers in Industry, *50*(3), 319–331. https://doi.org/10.1016/S0166-
3615(03)00019-8

Ding, S., Mannan, M. A., Poo, A. N., Yang, D. C. H., & Han, Z. (2003). Adaptive iso-
planar tool path generation for machining of free-form surfaces.

ElKott, D. F. (2007). *CAD-based CMM Inspection of Sculptured Surfaces*. Retrieved
from
https://books.google.ca/books/about/CAD_based_CMM_Inspection_of_Sculptured
_S.html?id=Rvjgmy4UEYEC&pgis=1

Chang.Kuang-Hua. (2015). 3 tool path.pdf. In *Product Manufacturing and Cost
Estimating Using CAD/CAE: The Computer Aided Engineering Design Series*.

Lasemi, A., Xue, D., & Gu, P. (2010). Recent development in CNC machining of
freeform surfaces: A state-of-the-art review. *CAD Computer Aided Design*.
https://doi.org/10.1016/j.cad.2010.04.002

Li, L. L., & Zhang, Y. F. (2004). Cutter Selection for 5-axis Milling based on Surface

Decomposition. *8th International Conference on Control, Automation, Robotics and Vision*, (December), 1863–1868.

Lin, Y. J., & Lee, T. S. (1999). Adaptive tool path generation algorithm for precision surface machining. *CAD Computer Aided Design*. https://doi.org/10.1016/S0010-4485(99)00024-X

Lin, Z., Fu, J., Shen, H., Gan, W., & Yue, S. (2015). Tool path generation for multi-axis freeform surface finishing with the LKH TSP solver. *CAD Computer Aided Design*. https://doi.org/10.1016/j.cad.2015.07.002

Liu, W., Zhou, L., & An, L. (2012). Constant scallop-height tool path generation for three-axis discrete data points machining. https://doi.org/10.1007/s00170-011-3892-3

Park, S. C., & Choi, B. K. (2001). Boundary extraction algorithm for cutting area detection, *33*, 571–579.

Radzevich, S. P. (2007). R-surfaces: A novel tool for partitioning of a sculptured surface. *Mathematical and Computer Modelling*, *46*(9–10), 1314–1331. https://doi.org/10.1016/j.mcm.2007.01.009

Roman, A., Bedi, S., & Ismail, F. (2006). Three-half and half-axis patch-by-patch NC machining of sculptured surfaces. *International Journal of Advanced Manufacturing Technology*, *29*(5–6), 524–531. https://doi.org/10.1007/BF02729105

Shunmugam, M. S. (1987). New approach for evaluating form errors of engineering surfaces. *Computer-Aided Design*, *19*(7), 368–374. https://doi.org/10.1016/0010-4485(87)90037-6

Obeidat S.M. (2008). *Adaptive Method for Form error determination in di*. University
of Oklahoma- Norman.

Xu, X. W., & Newman, S. T. (2006). Making CNC machine tools more open,
interoperable and intelligent - A review of the technologies. *Computers in
Industry*. https://doi.org/10.1016/j.compind.2005.06.002

Zhou, B., Zhao, J., & Li, L. (2015). CNC double spiral tool-path generation based on
parametric surface mapping. *CAD Computer Aided Design*.
https://doi.org/10.1016/j.cad.2015.06.005

APPENDICES

Appendix A: MATLAB® coding

Calculating Ruled and Free form surface equation

```matlab
syms u;
a = [u 1];
b = [-0.416 0.416;1 0];
c1 = [0 0.23 0; 2.4 0.65 0];
c2 = [0 0.75 3; 2.4 1.40 3];
first = a * b;
pu = first * c1;
qu = first * c2;
syms w;
sur_eqn = (1-w)*pu + w*qu;
N = 18;
u = linspace(0,2.4,N); % Plot points in U direction to 2.4
w = linspace(0,3,N); % Plot points in W direction to 3 inch
px = [0 2.4];
pz = [0.23 0.65];
py = [0 0];
qx = [0 2.4];
qz = [0.75 1.4];
qy = [3 3];
 % Plot points along U direction from 1 to 18


for i = 1:1:N
 Sx = (624*u(i)*w)/625 - (624*u(i)*(w - 1))/625;
 Sz = w*((169*u(i))/625 + 3/4) - ((546*u(i))/3125 + 23/100)*(w - 1);
 Sy = w.*ones(1,N);
 plot3(Sx,Sy,Sz)
 hold on
end
  % Plot points along W direction from 1 to 18
for i = 1:1:N
  Sx = (624*u*w(i))/625 - (624*u*(w(i)- 1))/625;
  Sz = w(i)*((169*u)/625 + 3/4) - ((546*u)/3125 + 23/100)*(w(i) - 1);
  Sy = w(i).*ones(1,N);
  plot3(Sx,Sy,Sz)
end

plot3(px,py,pz,'--')
hold on
plot3(qx,qy,qz,'--')
hold on

xlabel('x'),ylabel('y'),zlabel('z')
title('slope surface');
%view(-33, -65)
```

Free form surface 1: shallow

```matlab
syms u
b = [-1/6 1/2 -1/2 -1/6; 1 -15/6 2 -1/2; -11/6 3 -3/2 1/3; 1 0 0 0];
c = [u (1/10)*u^3-(21/40)*u^2+(5/8)*u+0.12 0;
    u (-2/25)*u^3+(7/25)*u^2-(3/25)*u+0.04 1;
    u (1/25)*u^3-(1/5)*u^2+(1/5)*u+0.2 2;
    u (-1/30)*u^3+(1/8)*u^2-(1/24)*u+0.05 3]; % Curve equation - p q r
syms w
a = [w^3 w^2 w 1];
first = a*b
surface_eqn = first*c % Lofted surface equation for curves p, q, r, t
N = 21;
u = linspace(0,3,N); % Plot points in U direction to 3 inch
w = linspace(0,3,N);  % Plot points in W direction to 3 inch
px = [0 1 2 3];
pz = [0.12 0.32 0.07 -0.03];
py = [0 0 0 0];
qx = [0 1 2 3];
qz = [0.04 0.12 0.28 0.04];
qy = [1 1 1 1];
rx = [0 1 2 3];
rz = [0.2 0.24 0.12 0.08];
ry = [2 2 2 2];
tx = [0 1 2 3];
tz = [0.05 0.1 0.2 0.15];
ty = [3 3 3 3];
 % Plot points along u direction from 1 to 21


for i = 1:1:N
  Sx = u(i)*(w.^3/2 - (5*w.^2)/2 + 3*w) - u(i)*(w.^3/2 - 2*w.^2 +
(3*w)/2) + u(i)*((w.^3)/6 - (w.^2)/2 + w/3) - u(i)*(w.^3/6 - w.^2 +
(11*w)/6 - 1);
  Sz = -(w.^3/2 - 2*w.^2 + (3*w)/2)*(u(i)^3/25 - u(i)^2/5 + u(i)/5 +
1/5) - (w.^3/6 - w.^2/2 + w/3)*(u(i)^3/30 - u(i)^2/8 + u(i)/24 - 1/20)
- (w.^3/2 - (5*w.^2)/2 + 3*w)*((2*u(i)^3)/25 - (7*u(i)^2)/25 +
(3*u(i))/25 - 1/25) - (u(i)^3/10 - (21*u(i)^2)/40 + (5*u(i))/8 +
3/25)*(w.^3/6 - w.^2 + (11*w)/6 - 1);
  Sy = w.*ones(1,N);
  plot3(Sx,Sy,Sz)
  hold on
end
 % Plot points along v direction from 1 to 21
for i = 1:1:N
  Sx = u*(w(i)^3/2 - (5*w(i)^2)/2 + 3*w(i)) - u*(w(i)^3/2 - 2*w(i)^2 +
(3*w(i))/2) + u*(w(i)^3/6 - w(i)^2/2 + w(i)/3) - u*(w(i)^3/6 - w(i)^2
+ (11*w(i))/6 - 1);
  Sz = -(w(i)^3/2 - 2*w(i)^2 + (3*w(i))/2)*(u.^3/25 - u.^2/5 + u/5 +
1/5) - (w(i)^3/6 - w(i)^2/2 + w(i)/3)*(u.^3/30 - u.^2/8 + u/24 - 1/20)
- (w(i)^3/2 - (5*w(i)^2)/2 + 3*w(i))*((2*u.^3)/25 - (7*u.^2)/25 +
(3*u)/25 - 1/25) - (u.^3/10 - (21*u.^2)/40 + (5*u)/8 + 3/25)*(w(i)^3/6
- w(i)^2 + (11*w(i))/6 - 1);
  Sy = w(i).*ones(1,N);
  plot3(Sx,Sy,Sz)
```

```matlab
    hold on
end

plot3(px,py,pz,'--')
hold on
plot3(qx,qy,qz,'--')
hold on
plot3(rx,ry,rz,'--')
hold on
plot3(tx,ty,tz,'--')

xlabel('x'),ylabel('y'),zlabel('z')
title('loft surface');
view(-33, 65)
```

Free form surface: 2: Deep

```matlab
syms u
b = [-1/6 1/2 -1/2 -1/6; 1 -15/6 2 -1/2; -11/6 3 -3/2 1/3; 1 0 0 0];
c = [u (1/10)*u^3-(21/40)*u^2+(5/8)*u+0.12 0;
    u (-2/25)*u^3+(7/25)*u^2-(3/25)*u+0.04 1;
    u (1/25)*u^3-(1/5)*u^2+(1/5)*u+0.2 2;
    u (-1/30)*u^3+(1/8)*u^2-(1/24)*u+0.05 3]; % Curve equation - p q r
and t
syms w
a = [w^3 w^2 w 1];
first = a*b;
surface_eqn = first*c; % surface equation for curves p, q, r and t
N = 21;
u = linspace(0,3,N);
w = linspace(0,3,N);
px = [0 1 2 3]; % curve p points
pz = [0.12 0.32 -0.20 -0.03];
py = [0 0 0 0];
qx = [0 1 2 3]; % curve q points
qz = [0.04 -0.32 0.28 0.24];
qy = [1 1 1 1];
rx = [0 1 2 3]; % curve r points
rz = [0.2 0.24 0.-30 0.08];
ry = [2 2 2 2];
tx = [0 1 2 3]; % curve t points
tz = [-0.05 0.1 0.25 -0.15];
ty = [3 3 3 3];
%%
% Plot points along u direction from 1 to N
for i = 1:1:N
  Sx = u(i)*(w.^3/2 - (5*w.^2)/2 + 3*w) - u(i)*(w.^3/2 - 2*w.^2 +
(3*w)/2) + u(i)*((w.^3)/6 - (w.^2)/2 + w/3) - u(i)*(w.^3/6 - w.^2 +
(11*w)/6 - 1);
  Sz = -(w.^3/2 - 2*w.^2 + (3*w)/2)*(u(i)^3/25 - u(i)^2/5 + u(i)/5 +
1/5) - (w.^3/6 - w.^2/2 + w/3)*(u(i)^3/30 - u(i)^2/8 + u(i)/24 - 1/20)
- (w.^3/2 - (5*w.^2)/2 + 3*w)*((2*u(i)^3)/25 - (7*u(i)^2)/25 +
(3*u(i))/25 - 1/25) - (u(i)^3/10 - (21*u(i)^2)/40 + (5*u(i))/8 +
3/25)*(w.^3/6 - w.^2 + (11*w)/6 - 1);
```

```matlab
  Sy = w.*ones(1,N);
  plot3(Sx,Sy,Sz)
  hold on
end

% Plot points along w direction from 1 to N
for i = 1:1:N
  Sx = u*(w(i)^3/2 - (5*w(i)^2)/2 + 3*w(i)) - u*(w(i)^3/2 - 2*w(i)^2 +
(3*w(i))/2) + u*(w(i)^3/6 - w(i)^2/2 + w(i)/3) - u*(w(i)^3/6 - w(i)^2
+ (11*w(i))/6 - 1);
  Sz = -(w(i)^3/2 - 2*w(i)^2 + (3*w(i))/2)*(u.^3/25 - u.^2/5 + u/5 +
1/5) - (w(i)^3/6 - w(i)^2/2 + w(i)/3)*(u.^3/30 - u.^2/8 + u/24 - 1/20)
- (w(i)^3/2 - (5*w(i)^2)/2 + 3*w(i))*((2*u.^3)/25 - (7*u.^2)/25 +
(3*u)/25 - 1/25) - (u.^3/10 - (21*u.^2)/40 + (5*u)/8 + 3/25)*(w(i)^3/6
- w(i)^2 + (11*w(i))/6 - 1);
  Sy = w(i).*ones(1,N);
  plot3(Sx,Sy,Sz)
  hold on
end

plot3(px,py,pz,'--');
hold on
plot3(qx,qy,qz,'--');
hold on
%plot3(rx,ry,rz,'--'); % Surface becomes plane if this line is
executed
%hold on
plot3(tx,ty,tz,'--');

xlabel('x'),ylabel('y'),zlabel('z')
title('loft surface');
```

Algorithm: For Region separation – Shallow

```matlab
clear;
tic;
syms u w;
% Parametric equation in U and W form

Sx = u*(w^3/2 - (5*w^2)/2 + 3*w) - u*(w^3/2 - 2*w^2 + (3*w)/2) +
u*((w^3)/6 - (w^2)/2 + w/3) - u*(w^3/6 - w^2 + (11*w)/6 - 1);
Sz = -(w^3/2 - 2*w^2 + (3*w)/2)*(u^3/25 - u^2/5 + u/5 + 1/5) - (w^3/6
- w^2/2 + w/3)*(u^3/30 - u^2/8 + u/24 - 1/20) - (w^3/2 - (5*w^2)/2 +
3*w)*((2*u^3)/25 - (7*u^2)/25 + (3*u)/25 - 1/25) - (u^3/10 -
(21*u^2)/40 + (5*u)/8 + 3/25)*(w^3/6 - w^2 + (11*w)/6 - 1);
Sy = w;
d1rzu=diff(Sz,'u',1);% first derivative of Z with respect to "U"
d1rzw=diff(Sz,'w',1);% first derivative of Z with respect to "W"
r=[Sx;Sy;Sz];
d1rw=diff(r,'w',1); % First derivative of the surface equation with
respect to "W"
d2rw=diff(r,'w',2); % Second derivate of the surface equation with
respect to "W"
```

```matlab
d1r=diff(r,'u',1); % First derivative of the surface equation with
respect to "U"
d2r=diff(r,'u',2); % Second derivative of the surface with respect to
"U"
d1ruw=diff(d1r,'w',1); %First derivative of the surface with respect
to "W"
F=cross(d1r,d2r);
F1=cross(d1r,d1rw);
n=F1/sqrt(sum(F1.^2));% normal vector on the surface
l=dot(n,d2r);
m=dot(n,d1ruw);
h=dot(n,d2rw);
e=dot(d1r,d1r);
f=dot(d1r,d1rw);
g=dot(d1rw,d1rw);
KC =(l*h -m^2)/(e*g-f^2);    % Gaussian curvature
H=1/2*((e*h -2*f*g)/(e*g-f^2)); % Mean curvature
c=1;
emptygc=[]; % initial empty matrix to store the Gaussian curvature
emptymean=[]; % initial empty matrix to store the Mean curvature

for u=0:0.05:3 % U value ranges from o to 3 on the increment of 0.05
    r=1;
    for w=0:.05:3

% GC equation and Mean equation should be given here %

emptygc(r,c)=gc;
emptymean(r,c)=mean;
 r=r+1;
    end
    c=c+1;
end
emptyM1=[];% Matrix M for storing the GC and Mean curvature value
m=1;
o=1;

% Conditions for grouping the Gaussian points and Mean points

for m=1:61
    for o=1:61
        if emptygc(m,o)>=0 && emptymean(m,o)<0 % Condition to store
the Convex and Plane points
        emptyM1(m,o)=1;
        else if emptygc(m,o)>=0 && emptymean(m,o)>0 % Condition to
store the Concave points
        emptyM1(m,o)=2;
        else
        emptyM1(m,o)=3; % condition to store the Saddle points
        end


        end
    end
end
```

NOMENCLATURE

CCx = cutter contact point in X direction

CLx = cutter location point in X direction

CCy = cutter contact point in Y direction

CLy = cutter location point in Y direction

CCz = cutter contact point in Z direction

CLz = cutter location point in Z direction

U $\quad$ = Parameter in X direction

W $\quad$ = Parameter in Y direction

N $\quad$ = spindle speed

F $\quad$ = feed rate

n $\quad$ = number of teeth

F_t $\quad$ = feed per teeth

D $\quad$ = Tool diameter

V $\quad$ = Cutting speed

H $\quad$ = Scallop height

S $\quad$ = step over

Γ $\quad$ = slope angle of the design surface

Oi $\quad$ = offset in X, Y, Z direction

T_W $\quad$ = Tangent point in W direction

T_U $\quad$ = Tangent point in U direction

R $\quad$ = Radius of the cutter

Ni $\quad$ = Tool orientation in X, Y, Z direction

Appendix B: Ruled surface measuring points

CMM actual measured			Calculated ideal Points		
X(inch)	Y(inch)	Z(inch)	X(inch)	Y(inch)	Z(inch)
2.0429	0.2427	0.8109	2.0419	0.2447	0.81
2.0388	0.6675	0.7332	2.0377	0.665	0.7312
2.0341	1.1458	0.6457	2.0321	1.1478	0.64
2.0309	1.4754	0.5854	2.0319	1.4754	0.454
2.0258	1.9939	0.4903	2.016	1.9769	0.5
2.022	2.3866	0.4182	2.02	2.356	0.4282
2.0174	2.861	0.3314	2	2.881	0.3321
1.446	2.8554	0.4341	1.4424	2.855	0.4321
1.4515	2.2904	0.5487	1.4545	2.315	0.522
1.4555	1.8737	0.633	1.45	1.8654	0.6312
1.4611	1.3013	0.7486	1.463	1.209	0.752
1.4646	0.9484	0.8199	1.465	0.9487	0.829
1.4679	0.607	0.8884	1.458	0.6	0.883
1.4709	0.296	0.9509	1.451	0.295	0.9785
1.0198	0.2916	1.0703	1.0123	0.2945	1.053
1.0155	0.734	0.9751	1.015	0.7344	0.9651
1.011	1.1883	0.877	1.01	1.1895	0.8677

1.004	1.9056	0.7217	1	1.9025	0.725
1.0001	2.3028	0.6355	1	2.318	0.6255
0.9948	2.8375	0.5195	0.995	2.8325	0.5255
0.505	2.8328	0.61	0.5	2.8312	0.6
0.5114	2.1644	0.7657	0.5024	2.1657	0.7695
0.5158	1.7172	0.8695	0.5148	1.7248	0.8595
0.5216	1.1194	1.008	0.5228	1.1184	1
0.5255	0.7286	1.0986	0.5251	0.7216	1.092
0.5286	0.4084	1.1726	0.5262	0.4025	1.1666
0.1799	0.4049	1.2638	0.178	0.4027	1.268
0.1751	0.8955	1.1449	0.175	0.955	1.1349
0.1691	1.4978	0.9988	0.1678	]1.5	1
0.1629	2.1345	0.8441	0.1665	2.198	0.851
0.1574	2.7005	0.7057	0.1554	2.7	0.7

Appendix C: Free from surface1-sample 3 measurement points

CMM measured points			Calculated Points		
X (inch)	**Y (inch)**	**Z (inch)**	**X (inch)**	**Y (inch)**	**Z (inch)**
2.5977	0.2017	1.3045	2.5954	0.2029	1.3041
2.0915	0.2013	1.2495	2.0936	0.2023	1.2495
1.3961	0.1777	1.2781	1.3969	0.1802	1.2786
0.7163	0.1768	1.2475	0.7177	0.1791	1.2486
0.2861	0.3219	1.1731	0.2882	0.3205	1.1735
0.8598	0.5171	1.3835	0.8581	0.5157	1.3826
1.4327	0.5435	1.3634	1.4313	0.5416	1.3635
1.8022	0.6842	1.2856	1.8017	0.6827	1.2856
2.3182	0.6848	1.2786	2.3182	0.6834	1.2785
2.318	1.0074	1.3019	2.3179	1.0068	1.3018
2.0918	0.9989	1.283	2.0927	1.001	1.2833
1.4747	1.0527	1.394	1.4753	1.051	1.3938
0.8129	1.0519	1.4283	0.814	1.0504	1.4284
0.3761	1.2072	1.3298	0.3772	1.2059	1.3298
0.8781	1.3138	1.4235	0.8777	1.3136	1.4234
1.3306	1.3144	1.4106	1.3306	1.3141	1.4106
1.8073	1.3293	1.3421	1.8072	1.3276	1.342
2.3552	1.4466	1.3441	2.355	1.4462	1.3441

1.5571	1.5383	1.3735	1.5572	1.5367	1.3735
0.6936	1.5373	1.3882	0.6934	1.5357	1.3883
0.2358	1.8525	1.4281	0.2365	1.8526	1.428
0.5225	1.9555	1.3819	0.5221	1.9555	1.382
0.9228	1.956	1.3179	0.9218	1.956	1.318
1.634	2.0631	1.3659	1.6341	2.0618	1.3659
2.4767	2.1531	1.3726	2.4759	2.1516	1.3727
2.0009	2.2233	1.4204	2.0011	2.222	1.4203
1.788	2.2231	1.3945	1.7883	2.2217	1.3946
1.2556	2.3085	1.2664	1.2562	2.3076	1.2665
0.7977	2.4828	1.2482	0.7986	2.4826	1.248
1.1233	2.729	1.2056	1.1225	2.7288	1.2055
1.5877	2.7296	1.3265	1.5876	2.7294	1.3264
2.0355	2.7301	1.4168	2.0359	2.7299	1.4169
2.4236	2.7306	1.377	2.4228	2.7303	1.3772
2.6771	2.7308	1.3109	2.677	2.7306	1.3109
0.2124	2.3358	1.4588	0.2126	2.3379	1.458
0.5895	2.1301	1.3541	0.5896	2.1308	1.354
0.9984	2.0494	1.294	0.9978	2.0513	1.2937
1.745	1.8916	1.3795	1.7444	1.8931	1.3795
2.2416	1.5373	1.3518	2.2405	1.5379	1.3518
1.7266	1.1951	1.3439	1.7266	1.1957	1.3439

1.0908	1.1944	1.444	1.0911	1.195	1.4439
1.0911	0.7859	1.4491	1.0915	0.7866	1.4491
1.0918	0.1452	1.2725	1.0922	0.146	1.2728
0.3963	0.1443	1.1842	0.3964	0.1452	1.1842
0.1145	0.7845	1.1881	0.1169	0.7844	1.1886
0.1136	1.6564	1.4644	0.1159	1.6483	1.4624
0.2494	2.255	1.4511	0.2473	2.2549	1.4516
0.8373	2.968	1.1971	0.8361	2.968	1.1971
0.2301	2.9675	1.3009	0.2304	2.9673	1.3009
1.9334	2.9696	1.3806	1.933	2.9693	1.3806
2.501	2.9373	1.3477	2.5002	2.9395	1.347
2.7864	2.6703	1.2803	2.7855	2.6711	1.2805
2.7874	1.8219	1.3279	2.7864	1.8224	1.3279
2.8018	0.7081	1.4497	2.8018	0.7081	1.4497
2.8022	0.4758	1.3585	2.7997	0.4776	1.3583
2.0808	0.7358	1.2592	2.0113	0.7356	1.2591
1.6567	1.2081	1.3577	1.6574	1.2081	1.3575
1.4441	1.6265	1.3733	1.4456	1.6265	1.3732
1.8527	1.8427	1.3845	1.8525	1.8426	1.3845

Appendix D: Free from surface2 -sample3

CMM Measured points			Calculated points		
X (inch)	**Y (inch)**	**Z (inch)**	**X (inch)**	**Y (inch)**	**Z (inch)**
2.6664	0.0606	0.9509	2.6661	0.0609	0.9514
2.3146	0.3679	1.1465	2.3142	0.3677	1.1465
2.894	0.8232	1.277	2.8941	0.8232	1.2774
2.2156	1.2371	1.3148	2.2156	1.2389	1.3145
2.4554	1.5612	1.2213	2.4553	1.561	1.2216
2.8493	1.742	1.1224	2.8593	1.7423	1.1229
2.5062	2.1573	1.038	2.5062	2.1552	1.04
2.9228	2.4317	0.9775	2.9228	2.4315	0.9872
2.0611	3.0531	1.19	2.0621	3.0394	1.156
0.8742	3.0396	1.034	0.8744	3.0385	1.036
0.2906	2.7311	1.0686	0.2911	2.7315	1.0679
0.3099	2.0904	1.234	0.3041	2.0909	1.2344
0.121	1.1717	0.9194	0.126	1.172	0.9195
0.6183	0.973	0.5945	0.6185	0.9735	0.5947
0.6633	2.0239	1.2385	0.6632	2.0239	1.2386
0.3646	0.1521	1.2144	0.3645	0.1521	1.2145
1.4722	0.1782	1.1877	1.4722	0.1782	1.2149
1.5675	0.8114	1.0239	1.5677	0.8147	1.0965
0.9063	1.4841	0.8416	0.9065	1.4841	0.8418

1.7109	1.6363	1.0715	1.7111	1.6364	1.0715
1.1386	2.0764	1.2275	1.1384	2.0764	1.2277
0.6674	2.8779	1.0565	0.6677	2.878	1.0568
2.1995	2.7899	1.227	2.199	2.7899	1.2269
0.1887	0.8775	0.8282	0.1886	0.8775	0.8285
0.2332	1.3116	0.8596	0.23325	1.3115	0.859
0.2638	0.1343	1.1916	0.2636	0.1343	1.1914
0.2775	2.9733	0.949	0.2776	2.9735	0.9495
0.6809	2.9274	1.0361	0.6807	2.9283	1.037
2.0798	2.0976	1.0896	2.0785	2.0777	1.0875
1.8581	1.5113	1.1118	1.8581	1.51128	1.1114
1.5368	1.4598	0.9946	1.5366	1.459	0.9956
1.0892	1.3637	0.7908	1.089	1.3631	0.7901
0.7461	1.1815	0.6127	0.7451	1.1814	0.6129
0.1941	1.1621	0.8372	0.1942	1.1622	0.8372
0.1959	0.6723	0.8918	0.196	0.6715	0.8917
0.4564	0.2468	1.1833	0.4559	0.2465	1.1835
1.1204	0.1925	1.2337	1.1204	0.1925	0.2336
1.8442	0.3299	1.1398	1.8446	0.3289	1.1397
1.8393	0.7618	1.1708	1.835	0.7614	1.1706
1.852	1.1843	1.1554	1.8521	1.1846	1.1559
2.2989	1.1894	1.3526	2.279	1.1895	1.3546

2.7522	1.3183	1.3112	2.7527	1.3173	1.3115
2.7626	0.4532	1.1711	2.7636	0.4544	1.1719
2.2049	0.1568	1.0486	2.2055	0.1564	1.0481
1.4211	0.1479	1.2016	1.4215	0.1477	1.2016
1.2959	2.1296	1.2229	1.296	2.1295	1.123
0.6548	2.1223	1.2645	0.6547	2.1228	1.2649
0.2585	2.0251	1.2163	0.2582	2.0254	1.2167
0.25	2.7771	1.0411	0.2541	2.7776	1.2165
1.186	2.7878	1.1924	1.1896	2.7882	1.1945
2.0556	2.7967	1.2458	2.0564	2.7966	1.1965
2.3194	2.3056	1.0932	2.3199	2.3065	1.0937
2.5765	1.7705	1.1194	2.5755	1.7704	1.1194
2.5847	1.0599	1.4035	2.5846	1.0594	1.4035
2.78	0.293	1.0777	2.7821	0.2945	1.0774
2.7576	2.2872	1.0148	2.7586	2.2875	1.0144
1.7204	2.2301	1.1806	1.7215	2.2312	1.1807
0.9772	2.1772	1.2649	0.9776	2.1774	1.2634
0.2457	2.1688	1.2278	0.2455	2.1689	1.2275